

Compact stub-loaded open-loop BPF with enhanced stopband by introducing extra transmission zeros

Nagendra Kumar and Yatendra Kumar Singh

Open-loop resonators (OLRs) are loaded with one or two stubs to design a compact bandpass filter (BPF) with a wide stopband by creating extra transmission zeros. By properly selecting the length of the stubs and their positions, extra transmission zeros are created in the stopband before the spurious passband, thus giving wide stopbands. Mathematical analyses are performed to show the effect of open stubs on the OLR. A two-stub-loaded BPF is designed and fabricated, which shows a harmonic suppression of up to $3.2f_o$ by creating five transmission zeros and 44% size reduction as compared with a simple OLR-based filter without stubs. Measured results are in good agreement with the theoretical analysis and simulation results.

Introduction: Several efforts have been reported to design a compact open-loop bandpass filter (BPF) having better harmonic suppression. Stubs and lumped elements are loaded to the centre of the open-loop resonators (OLRs) to suppress spurious responses in [1, 2], respectively. However, centre loading does not lead to compactness because it has a minimum effect on the centre frequency. In [3], coupled open stubs are introduced in OLRs to suppress the second harmonic with a size reduction of 20.3%. Spurious suppression by properly selecting the coupling regions between shorted and OLRs are reported in [4]. Also, multiple transmission zeros are created in the stopband to suppress harmonics in [5–7]. However, except [6, 7] are larger in size.

In this Letter, we present a novel application of stub(s) to design compact BPFs that have extra transmission zeros in the stopband, created due to the stubs and their positions.

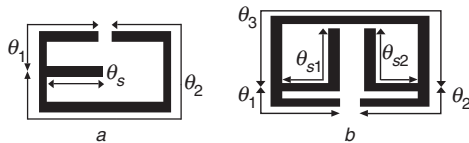


Fig. 1 Single stub-loaded resonator and two-stub-loaded resonator

a Single stub-loaded
b Two-stub-loaded

Stub(s)-loaded OLR: The single stub-loaded OLR is shown in Fig. 1a. The input impedance looking from one open end can be written as

$$Z_{in} = jZ_o \frac{\tan \theta_1 \tan \theta_2 + \tan \theta_1 \tan \theta_s - 1}{\tan \theta_1 + \tan \theta_2 + \tan \theta_s} \quad (1)$$

For resonance

$$Z_{in} = \infty \quad (2)$$

Hence, the condition for resonance can be deduced from (1) as

$$\tan(\theta_1) + \tan(\theta_2) + \tan(\theta_s) = 0 \quad (3)$$

For the desired value of frequency f_o , electrical lengths θ_1 and θ_2 can be determined for a fixed value of θ_s . The centre frequency of an OLR loaded with an open stub (except centre loading) shifts to a lower value compared with the simple OLR without any stub due to increase in the electrical length or increase in the capacitive loading. In addition to reducing the centre frequency, the stub and its placement create a transmission zero in the frequency response before the second harmonic, thus widening of the stopband is achieved. Moreover, the transmission zero provides better rejection close to the desired frequency. Similar to (3), the resonance condition of a two-stub-loaded OLR as shown in Fig. 1b can be written as

$$\begin{aligned} &\tan(\theta_1) + \tan(\theta_2)\tan(\theta_3) + \tan(\theta_{s1}) + \tan(\theta_{s2}) \\ &- \tan(\theta_1)\tan(\theta_2)\tan(\theta_3) - \tan(\theta_1)\tan(\theta_3)\tan(\theta_{s2}) \\ &- \tan(\theta_2)\tan(\theta_3)\tan(\theta_{s1}) - \tan\theta_3\tan(\theta_{s1})\tan(\theta_{s2}) = 0 \end{aligned} \quad (4)$$

More lowering of the centre frequency can be achieved with respect to the single stub-loaded OLR due to more capacitive loading.

Analysis of single stub-loaded open-loop filter with 0° feeding: The schematic of the single stub-loaded open-loop filter with a 0° feed configuration is depicted in Fig. 2. The signal entering from the input has two paths, M_1 and M_2 , to the output as shown in Fig. 2. Each signal path contains microstrip line sections of lengths l_a , l_b and l_d and a coupled section of length l_c .

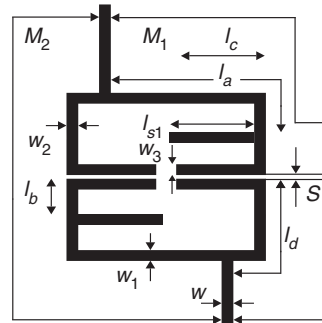


Fig. 2 Single stub-loaded open-loop filter

The $ABCD$ matrix of paths M_1 and M_2 can be written as

$$M_1 = \begin{bmatrix} A_1 & B_1 \\ C_1 & D_1 \end{bmatrix}_{\text{stub}_1} = M_a M_{s1} M_b M_c M_d \quad (5)$$

$$M_2 = \begin{bmatrix} A_2 & B_2 \\ C_2 & D_2 \end{bmatrix}_{\text{stub}_1} = M_d M_c M_b M_{s1} M_a \quad (6)$$

where M_a , M_b and M_d are the $ABCD$ matrices of a transmission line of length l_a , l_b and l_d respectively. M_{s1} and M_c are the $ABCD$ matrices of an open stub of length l_{s1} and lossless parallel coupled microstrip lines of length l_c , having both ends open on the same side, respectively. As two paths M_1 and M_2 are in parallel, the equivalent Y -matrix is the sum of the Y -matrices of each path. Finally, the Y -matrix of each path is calculated by converting the $ABCD$ parameter obtained in (5) and (6). The S_{21} and S_{11} of the whole circuit can be calculated from the equivalent Y -matrices of the two parallel paths. Fig. 3 compares two responses of single stub-loaded OLR designed for the same resonating frequency, $f_o = 1.82$ GHz, having an equal stub length of $\theta_s = 40^\circ$ with different position θ_1 from the open end. The filter is designed on an RT/Duroid 6010.2 substrate with $h = 0.635$ mm and $\epsilon_r = 10.2$. The length of different sections of the OLRs can be evaluated from (3). By solving

$$\text{Abs}[S_{21}] = 0 \quad (7)$$

the frequency of the transmission zeros can be determined. While solving (7) using Mathematica numerically, the right-hand side is replaced by a very small number, e.g. 10^{-5} or smaller. Hence, at $\theta_1 = 34^\circ$ the first two roots of (7) are the frequencies of two transmission zeros TZ_1 and TZ_2 which are due to the 0° feeding. The third root gives the frequency of transmission zero, TZ_3 , located before the second harmonic. Hence, the above analysis including a coupled line is very useful to obtain the harmonic response of the circuit compared with [1] where analysis only plots the relationship between the resonating frequency and the second harmonic. At $\theta_1 = 34^\circ$, the second harmonic comes after TZ_3 but at $\theta_1 = 22^\circ$ it shifts after the fourth transmission zero, TZ_4 , and thus gives a wider separation. Hence this extra transmission zero, TZ_4 , which appears due to the position of the stub, leads to a wider stopband in the response without increasing the size of the filter.

Two-stub-loaded OLR: The approach is further extended to achieve an even wider stopband by placing two stubs as shown in Fig. 4. The $ABCD$ matrix of the two paths can be written as

$$M_1 = M_a M_{s1} M_b M_c M_e M_{s2} M_d \quad (8)$$

$$M_2 = M_d M_{s2} M_e M_c M_b M_{s1} M_a \quad (9)$$

where M_{s1} and M_{s2} are the two-stub matrices for lengths l_{s1} and l_{s2} . Similar to the previous conclusions, two different stubs having different positions from open ends create two transmission zeros at two different positions. One more transmission zero can be achieved by the proper placement of stubs, which leads to more rejection. Use of the second stub in the design also leads to a further decrease in the size of the

BPF. Further compactness can be achieved by changing the width of various parts of the OLRs. The condition, $w_3 > w_2 > w_1$, shifts the centre frequency to a more lower value.

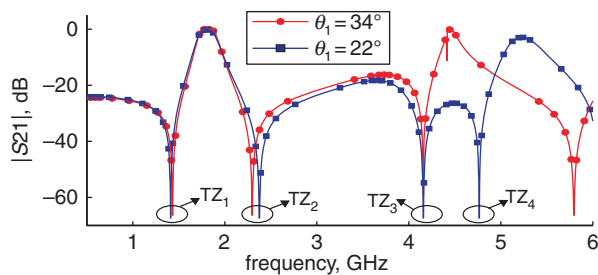


Fig. 3 Theoretical responses of single stub-loaded OLR with different θ_1

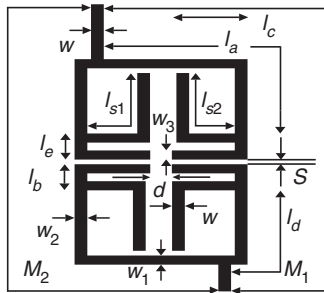


Fig. 4 Two-stub-loaded OLR-based filter

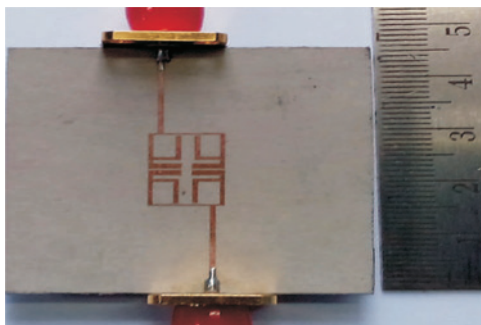


Fig. 5 Fabricated filter

$l_a = 10.5$, $l_b = 0.9$, $l_c = 3.5$, $l_d = 5.64$, $l_e = 0.86$, $l_{s1} = 6.8$, $l_{s2} = 6.5$, $s = 0.24$, $d = 1$, $w = 0.59$, $w_1 = 0.2$, $w_2 = 0.5$ and $w_3 = 1.0$, all in mm

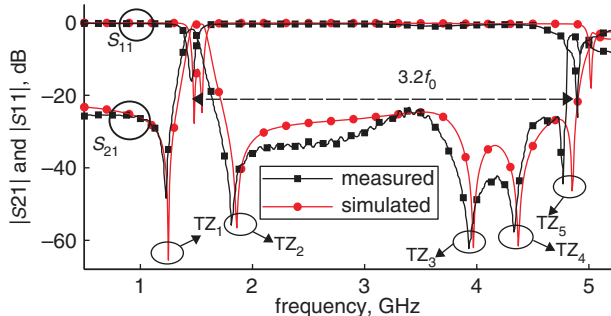


Fig. 6 Measured and simulated responses of two-stub-loaded open-loop filter

Fabrication and measurement: A second-order filter consisting of two-stub-loaded OLRs centred at 1.46 GHz having 3 dB fractional

bandwidth of 9%, is designed and fabricated. Equation (4) is used to design the filter. Gap, s , between the two resonators and the tapping point is calculated from the required coupling-coefficient and quality factor, respectively. The fabricated filter and the response, are shown in Fig. 5 and Fig. 6, respectively. The response of the BPF having two stubs of different lengths is plotted in Fig. 6. The transmission zeros TZ_1 and TZ_2 are at the passband edges at 1.25 and 1.86 GHz, respectively. Two transmission zeros TZ_3 and TZ_4 at 3.93 and 4.33 GHz, respectively, are due to the two different stub lengths. The additional transmission zero TZ_5 at 4.89 GHz is due to their proper positioning.

Comparison: The proposed filter is 44% more compact than a second-order filter using simple OLRs or OLRs loaded with stubs or lumped elements at the centre [1, 2]. Table 1 compares the current and previous works. The first and second works consist of OLRs with uniform and non-uniform widths, respectively.

Table 1: Comparison with previous reported works

Reference	Cent. freq. f_0 (GHz)	Size λ_{g0}^2	Trans. zeros	Stopband suppression level
[4]	0.97	0.27×0.13	3	22 dB up to $2f_0$
[2]	1.18	0.25×0.13	3	20 dB up to $2.5f_0$
[5]	2.4	0.16×0.11	5	20 dB up to $4f_0$
[7]	2.0	0.51×0.39	7	27 dB up to $2.88f_0$
[6]	3.0	0.35×0.29	6	15 dB up to $2.72f_0$
This work $w_1 = w_2 = w_3 = 0.59$ mm Fig. 5	1.63	0.18×0.11	5	25 dB up to $3.0f_0$
	1.46	0.17×0.1	5	26 dB up to $3.2f_0$

Conclusion: This Letter describes the compactness and the creation of the transmission zeros due to the proper positioning of the stubs in the OLRs. The response of the fabricated filter is shown in Table 1. Higher-order BPFs can also be designed using the same topology.

© The Institution of Engineering and Technology 2015

7 October 2014

doi: 10.1049/el.2014.3523

One or more of the Figures in this Letter are available in colour online.

Nagendra Kumar and Yatendra Kumar Singh (Department of Electrical Engineering, Indian Institute of Technology Patna, Patna, Bihar, India)

E-mail: nagendra@iitp.ac.in

References

- Tu, W.-H., Li, H., Michalski, K.A., and Chang, K.: 'Microstrip open-loop ring bandpass filter using open stubs for harmonic suppression'. IEEE MTT-S Int. Microwave Symp. Digest, San Francisco, CA, USA, June 2006, pp. 357–360
- Zhang, X.Y., and Xue, Q.: 'Novel centrally loaded resonators and their applications to bandpass filters', *IEEE Trans. Microw. Theory Tech.*, 2008, **56**, (4), pp. 913–921
- Zhang, X.-Y., Xue, Q., and Hu, B.-J.: 'Novel bandpass filter with size reduction and harmonic suppression', *Microw. Opt. Technol. Lett.*, 2007, **49**, (4), pp. 914–916
- Dai, G.L., Zhang, X.Y., Chan, C.H., Xue, Q., and Xia, M.Y.: 'An investigation of open- and short-ended resonators and their applications to bandpass filters', *IEEE Trans. Microw. Theory Tech.*, 2009, **57**, pp. 2203–2210
- Torabi, A., and Forooraghi, K.: 'Miniature harmonic-suppressed microstrip bandpass filter using a triple-mode stub-loaded resonator and spur lines', *IEEE Microw. Wirel. Compon. Lett.* 2011, **21**, (5), pp. 255–257
- Feng, W., and Che, W.: 'Bandpass filter using open/shorted dual behaviour resonators', *Electron. Lett.*, 2014, **50**, (8), pp. 610–611
- Deng, P.-H., and Tsai, J.-T.: 'Design of microstrip cross-coupled bandpass filter with multiple independent designable transmission zeros using branch-line resonators', *IEEE Microw. Wirel. Compon. Lett.*, 2013, **23**, (5), pp. 249–251